Available online at www.sciencedirect.com
ScienceDirect
Carbohydrate Research 342 (2007) 954–960
Carbohydrate RESEARCH

Conformational changes in single carboxymethylcellulose chains on a highly oriented pyrolytic graphite surface under different salt conditions

Tomotsugu Ueno, Shingo Yokota, Takuya Kitaoka* and Hiroyuki Wariishi

Department of Forest and Forest Products Sciences, Graduate School of Bioresource and Bioenvironmental Sciences, Kyushu University, Fukuoka 812-8581, Japan

Received 17 December 2006; received in revised form 22 January 2007; accepted 25 January 2007
Available online 3 February 2007

Abstract—Conformational changes in individual carboxymethylcellulose (CMC) chains deposited on a highly oriented pyrolytic graphite (HOPG) surface were investigated by atomic force microscopy (AFM). A small amount of CMC solution with various salt concentrations was deposited onto the HOPG surface. The CMC molecular chains adsorbed onto the HOPG surface were clearly visualized using tapping-mode AFM under ambient conditions, as compared with those on a hydrophilic mica surface. Each CMC chain was distinguishable at the molecular level based on the vertical profiles of the AFM images, and probably aligned along the HOPG crystal lattice. Higher NaCl concentrations brought about dramatic conformational changes from aligned single chains to globular aggregates via the molecular network structure only on the HOPG surface through electrostatic screening of the CM groups. Although CMC is a water-soluble hydrophilic polyelectrolyte, some interaction, possibly due to a CH-π bonding between the glucopyranosic axial plane of CMC and the aromatic rings of HOPG, is considered to be effective and dominant for the unique molecular attachment. These phenomena would imply the potential use of HOPG as a substrate for not only molecular imaging, but also for nano-scale morphological control of cellulosic polymers and other structural polysaccharides.

Keywords: Carboxymethylcellulose; Chain conformation; Highly oriented pyrolytic graphite; Atomic force microscopy

1. Introduction

Atomic force microscopy (AFM) is a powerful tool for imaging single polymer chains on atom flat substrates at high resolution, especially in the vertical direction.[1] AFM can be used to visualize the real morphological information of polymer chains and their assembly, which is in general difficult to investigate by conventional instrumental analyses for polymer characterization, for example, light scattering photometry, viscoelastic measurement and size exclusion chromatography. This approach results in an average response based on large numbers of polymer molecules.[2] Hence, there are a lot of AFM studies on the nano-imaging of various polymer chains, for example, deoxyribonucleic acid (DNA), synthetic polymers, and polysaccharides.[3–5] Recently, it has been reported that successful AFM imaging requires appropriate interactions between the polymer chains and substrate in order to avoid the displacement and distortion of the polymer samples by the AFM probe tip.[2]

Individual DNA chains were successfully placed on a mica surface by electrostatic interaction through a simple deposition from an aqueous DNA solution containing divalent ions such as Ni(II).[6] Surface modification of mica with aminopropyltriethoxysilane or poly-L-ornithine was also reported for improving the affinity of DNA for the substrate.[7,8] The conformations of the immobilized DNA molecules on the mica surface are similar to those in solution, as determined from the

* Corresponding author. Tel./fax: +81 92 642 2993; e-mail: tkitaoka@agr.kyushu-u.ac.jp

0008-6215/$ - see front matter © 2007 Elsevier Ltd. All rights reserved.
doi:10.1016/j.carres.2007.01.017

results obtained by statistical structure analysis of the contour/persistent lines and end-to-end lengths of the observed DNA chains.[9] On the other hand, synthetic polymers such as *n*-alkane-grafted polymers, which are soluble in organic solvents, were epitaxially arrayed on a highly oriented pyrolytic graphite (HOPG) surface by hydrophobic interaction, and their crystal growth was successfully observed.[10–12] The polymer morphology found at a polymer/substrate interface can provide a significant insight into the fundamental knowledge of polymer characteristics, while being influenced by various factors: solution properties (pH, ionic strength, and temperature), substrate features (hydrophobicity, hydrophilicity, and surface charge) and the polymer characteristics themselves.

Carboxymethylcellulose (CMC), which is one of the major cellulose derivatives, is produced by heterogeneous etherification of solid cellulose with monochloroacetic acid.[13] CMC is a water-soluble polysaccharide and has wide application in cosmetics and foods as a water retention agent and a dispersion stabilizer, respectively. Various physicochemical properties of CMC solutions dependent on pH, ionic strength and temperature have been reported to date;[14–16] however single molecular behavior of CMC molecules has not yet been put into detailed investigation. Conformational changes in single CMC molecules would provide new information for understanding the molecular functions of cellulose-based polymers. In recent years, the water-soluble polysaccharides such as xanthan,[17] succinoglycan[18] and alginate[19] were successfully observed on a mica surface by utilizing hydrogen bonding between the hydroxyl groups in the polysaccharides and the thin water layer formed on the mica surface at a relative humidity around 50–60%. The conformation of such polysaccharides on the mica surface is similar to that in solution and comparable to DNA molecules immobilized on the mica surface. A similar approach was applied to observe single CMC chains;[20] however, uncontrollable aggregation of the CMC molecules occurred. CMC molecules have a heterogeneous molecular structure consisting both of amphipathic anhydrous glucopyranose (AHG; hydrophilic equatorial sides and a hydrophobic axial plane) and hydrophilic CM units. Therefore, it is difficult to obtain a clear image of single CMC chains due to insufficient molecular attachment on the mica substrate through weak CMC/mica interactions. Recently, hyaluronic acid (HA), a negatively charged polysaccharide, was successfully observed on an HOPG surface using AFM.[21] This report suggested that stronger interactions were possibly involved between HA-type polysaccharides and HOPG as compared to those between HA and mica (thin water layer).

In this study, single CMC chain conformation on the HOPG surface was investigated by tapping-mode AFM analysis under atmospheric conditions. The CMC/HOPG interactions were altered by changing the type and concentration of inorganic salts which were added into the CMC solution, and the observed morphological changes in the individual CMC chains are discussed.

2. Results and discussion

2.1. AFM imaging of CMC chains on mica and HOPG surfaces

The structure of CMC sodium salt used in this study is illustrated in Chart 1. Water-soluble CMC molecules were placed on a mica substrate by the simple deposition method according to a previous report.[2] Although this technique is applicable for many anionic polysaccharides,[17–19] nearly no CMC adsorption was observed (data not shown). As reported so far, this method is applied only to polyelectrolytes with a low charge density on account of the weak electrostatic repulsion toward the mica surface.[2] Thus, poor CMC attachment onto the mica indicated that a strong electrostatic repulsion possibly occurred at the CMC/mica interface. Adding $NiCl_2$ solution (final concentration: 10 mM) to shield such electrostatic repulsion according to the previous study on DNA observation[6] resulted in fibrous CMC aggregates on the mica surface (Fig. 1a). Part of the CMC chains had an approximate monomolecular height ranging from 0.7 to 1.2 nm, as shown in Figure 1b. It is well known that divalent cations act as electrostatic screening and bridging substances between anionic polymers and mica substrates.[6] In this case, enhancing the affinity of CMC for mica was achieved to some extent by the addition of Ni(II) salts. However, a precise

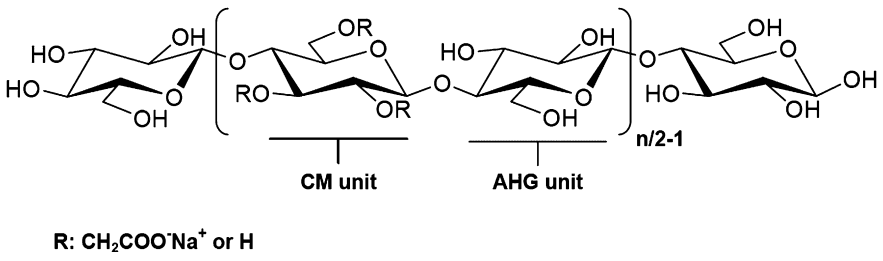

Chart 1. Chemical structure of CMC sodium salt used in this study.

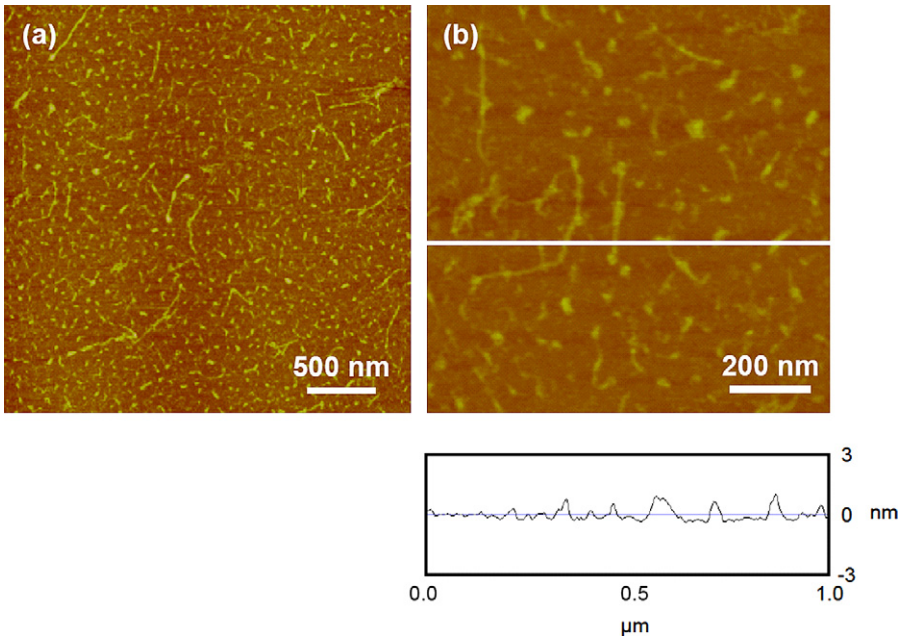

Figure 1. AFM images of CMC molecules on mica substrate treated with 10 mg L^{-1} of CMC solution containing 10 mM of $NiCl_2$: (a) wide region (3.0×3.0 μm^2), and (b) magnified image of (a) (1.0×1.0 μm^2) and height profile along the scanning line indicated in the image.

AFM analysis could not be carried out since such a weak attraction was difficult to reproducibly control with different salt types and/or concentrations; thus in this study, the conformational heterogeneity of CMC molecules was only observed.

CMC molecular chains deposited on an HOPG surface from a CMC solution with 10 mM NaCl are shown in Figure 2. A unique stretched wire-net morphology of highly oriented and extended CMC chains was clearly observed by tapping-mode AFM analysis. Figure 2c displays a height line profile of the cross section of Figure 2a, revealing a single chain (arrow #1; 1.10 nm) and two overlapped molecules (arrow #2; 2.19 nm), as indicated by the height being twice that of the single chain. These results suggested that the CMC molecular chains on the HOPG surface were well scattered at a mono-chain level

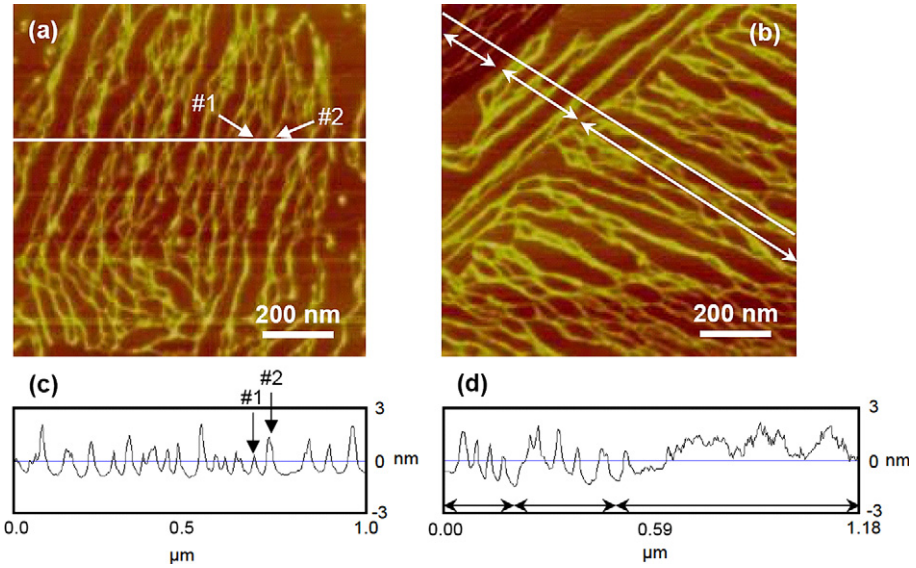

Figure 2. AFM images of CMC molecules on HOPG substrate: (a, b) HOPG surfaces treated with 10 mg L^{-1} of CMC solution containing 10 mM of NaCl, and (c, d) corresponding height profiles along the scanning line indicated in each image. In (a) and (c), arrow #1 indicates a CMC single chain and arrow #2 shows the crossing point of two single chains. In (b) and (d), double-headed arrows indicate the cross-sectional region of each HOPG layer.

and connected to each other.[22] Part of CMC chains had a folded conformation probably because the highly substituted CM units were more flexible than the AHG ones in the CMC chains with a heterogeneous molecular structure. Without salt addition, nearly no CMC adsorption was found on the HOPG surface, which is similar to the results of CMC adsorption on mica, possibly due to the strong electrostatic repulsion between the CMC molecules (data not shown). Besides, a successful AFM imaging could be achieved by adjusting a contact time of CMC droplet with the HOPG surface; a short contact for 3 s was the best condition in this study. In all cases for the AFM imaging, longer contact time brought about the excessive adsorption of CMC molecules and their assembly, resulting in an obscure molecular imaging because of the overall coverage of the HOPG surface. Hence, the unique alignment of CMC chains presumably occurred immediately after dropping the CMC solution on the HOPG surface. Figure 2b illustrates the high orientation of CMC molecules with different directions on the same HOPG surface. There were three HOPG layers in the scanning area of $1.0 \times 1.0\ \mu m^2$ (double-headed arrows correspond to each HOPG layer), and the CMC orientation obviously varied on each layer. The HOPG substrate used in this study had a polycrystalline structure with many layers accumulated one on top of the other. Therefore, these AFM images indicated that the CMC molecular chains were possibly aligned along the HOPG crystal lattice.

The CMC molecular chains existing on the HOPG surface showed highly extended conformation and in a unique array, which have not been observed with regard to HA molecules.[21] An epitaxial array of hydrophobic *n*-alkane crystals on hydrophobic HOPG has already been reported;[12] however in this study, water soluble (i.e., hydrophilic) CMC chains were arranged along the direction of the hydrophobic HOPG crystal lattice. The CMC molecules consist both of hydrophilic CM units and hydrophobic ribbon-shaped AHG units, as shown in Chart 1. It was reported that the hydrophobic axial plane of the AHG units of cellulose strongly interacts with the sp^2 hybridized orbital of the aromatic rings due to CH-π bonding.[23,24] Therefore, the residual AHG units in the CMC chains must play an important role in the CMC arrangement on the HOPG surface.

From the viewpoint of simple molecular observation, it may be considered that the CMC molecules deposited on the HOPG surface do not reflect their conformation in the solution state. On the mica surface, the CMC represented heterogeneous conformations (Fig. 1), while on the HOPG surface a specific conformation was observed (Fig. 2). Furthermore, all the height data of the CMC chains coincided well with ca. 1.1 nm on the HOPG surface, although the vertical profiles on mica showed some distribution (0.7–1.2 nm). A previous report concerning xanthan observation on mica discussed the unreliability of the vertical measurement of the deposited polymer chains,[17] because of the possibility that the polymers were compressed to some extent in the thin water layer formed on the mica surface. Thus, it was suggested that the AFM study of polysaccharide morphology on HOPG may be advantageous for precise vertical measurements of single polymer chains.

2.2. Conformational changes in CMC chains at different salt concentrations

The conformational changes in CMC chains were investigated in detail with regard to the addition of NaCl to the aqueous CMC solution. Figure 3 shows the CMC morphological changes induced by different NaCl concentrations. As compared to the AFM images shown in Figure 2 (NaCl; 10 mM), the CMC chains became densely entangled in the case of 15 mM of NaCl; the

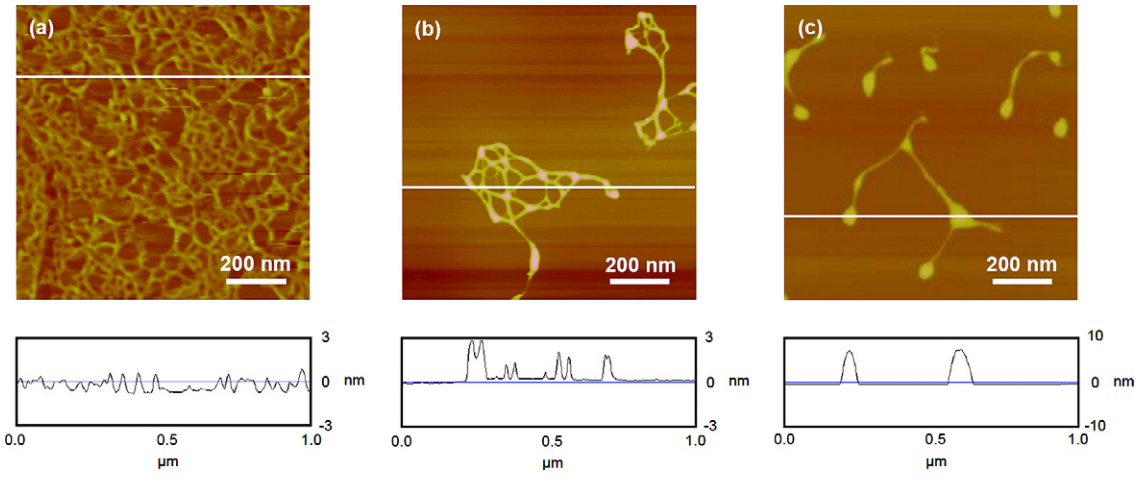

Figure 3. AFM images of CMC molecules on HOPG substrate: (a–c) HOPG surfaces treated with 10 mg L^{-1} of CMC solution containing NaCl: (a) 15 mM, (b) 20 mM, and (c) 50 mM. The corresponding height profiles of the CMC chains along the scanning line are indicated below each AFM image.

chain orientation became obscure and the molecular extension appeared to be relaxed, as shown in Figure 3a. Previous AFM studies on anionic polysaccharides also reported that the chain flexibility varied with the ionic strength of the polymer solution.[17–19] The height of the observed CMC chains was approximately maintained within the range from 1 to 2 nm, and thus the CMC network was regarded as single CMC chains and small bundles thereof. Higher NaCl concentrations resulted in aggregation of thicker CMC bundles with height ranging from 1 to 3 nm (Fig. 3b), and finally in the case of 50 mM NaCl, the formation of large globules with a height of more than 7 nm and a width from 70 to 100 nm (Fig. 3c). These morphological variations in the CMC chains at 0–50 mM NaCl concentration presumably reflected the changes in the CMC/CMC and CMC/HOPG interactions. Increasing the NaCl concentration from 0 to 10 mM triggered the adsorption of CMC molecules on the HOPG surface via an electrostatic screening of the CMC molecules; however, an adequate repulsion still remained. Further NaCl addition over 10 mM gradually emphasized the intermolecular CMC interaction by a counterion condensation effect.[17–19] Unique conformational changes of the CMC molecules, from aligned single chains to globular aggregates via the molecular network structure, were controllable only on the HOPG surface by simply adjusting the NaCl concentration in the CMC solution. Longer contact time of CMC droplet with the HOPG surface brought about the excessive surface coverage, while the observed CMC morphology remained almost unchanged. A successful visualization of such CMC conformational changes suggested that the unique interaction acting at the CMC/HOPG interface was relatively strong enough to adsorb, but not to the extent that intermolecular CMC association was masked.

2.3. Effect of salt types on CMC nano-morphology

Monovalent Na(I) ions had great impact on the CMC conformation and assembling features on the HOPG substrate. Subsequently, the nano-morphological behavior of CMC molecules was investigated using divalent ions: Ni(II) and Ca(II). In the case of the CMC solution containing a 0.5 mM $NiCl_2$ concentration, a clear adsorption of single CMC chains was observed as shown in Figure 4a. The CMC molecules showed a highly extended and oriented morphology similar to that observed at a NaCl concentration of 10 mM (Fig. 2). Further addition of Ni(II) ions resulted in a quick gathering of CMC molecules, and the formation of massive aggregates at a 10 mM $NiCl_2$ concentration (Fig. 4b). A contact time of CMC droplet with the HOPG surface was only 3 s, and thus it was presumed that the CMC aggregates formed in solution were attached on the HOPG surface as they were. When a hydrophilic mica substrate was used, the electrostatic shielding effect was not sufficient under the CMC solution conditions at 0.5 mM $NiCl_2$, such that no CMC adsorption occurred (data not shown). On the other hand, the molecular association of CMC chains on the HOPG surface at a higher $NiCl_2$ concentration was emphasized, as compared with that on mica (Fig. 2b). The addition of $CaCl_2$ also induced a similar nano-morphology of CMC chains, as shown in Figure 5. Therefore, divalent cations had a more powerful screening ability than monovalent ions. Ni(II) has an ionic radius of 0.69 Å, with respect to 0.99 Å of Ca(II),[6] and this size

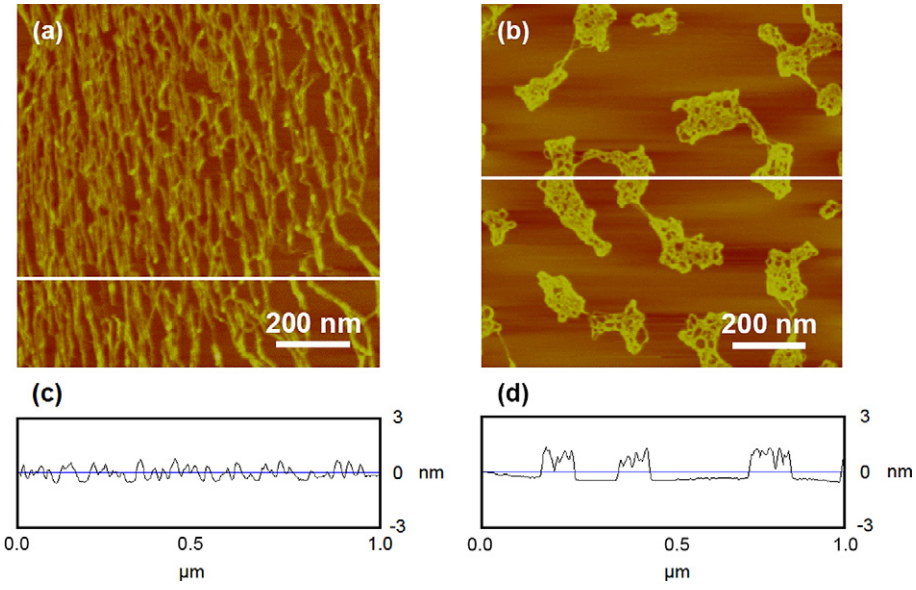

Figure 4. AFM images of CMC molecules on HOPG substrate: (a) 0.5 mM of $NiCl_2$, and (b) 10 mM of $NiCl_2$. The height profile of the CMC chains along the scanning line are indicated below each AFM image (c, d).

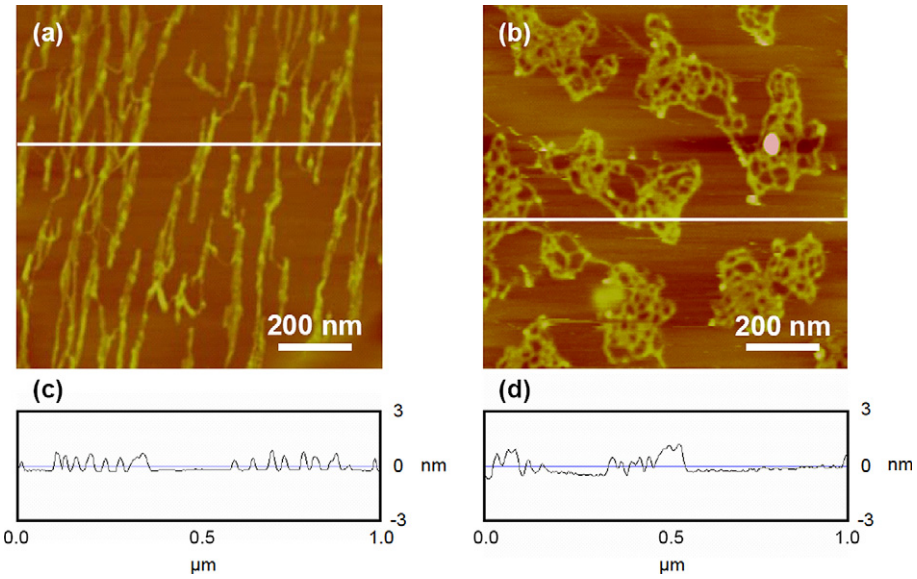

Figure 5. AFM images of CMC molecules on HOPG substrate: (a) 0.5 mM of $CaCl_2$, and (b) 10 mM of $CaCl_2$. The height profile of the CMC chains along the scanning line are indicated below each AFM image (c, d).

difference has often been discussed for explaining polyelectrolyte morphology on flat surfaces. In this study, the CMC nano-morphological behavior on the HOPG surface was not closely related to the ionic radius of the counterions for dissociated CM groups. However, the unique conformational changes in CMC molecular chains would imply the potential use of HOPG as substrate, for not only molecular imaging but also for nano-scale morphological control of functional polysaccharides that are expected to have some hydrophobic interaction at the HOPG interface.

3. Conclusion

Water-soluble CMC molecules were successfully immobilized on the hydrophobic HOPG surface by adding small amounts of Na(I), Ni(II) or Ca(II) ions into the CMC solution, and various CMC conformations were visualized by AFM analysis. The nano-morphology of the CMC chains varied according to the salt addition: mono-chain alignment, molecular network, bundles and globules. Such CMC conformations presumably depended on the hydrophobic interaction acting at the CMC/HOPG interface, and were controllable to some extent by the types of salts and concentrations used. The CMC molecular chains were well arranged along the crystalline orientation of the HOPG surface, and the hydrophobic AHG structure of the CMC molecules had a possible contribution to interact with the HOPG surface through a hydrophobic attraction. These results suggested the potential use of HOPG as substrate of choice for AFM observation and molecular alignment of individual cellulosic polymers and other polysaccharides.

4. Experimental

4.1. Materials

CMC sodium salt [degree of substitution: ca. 0.8, molecular weight: ca. 3×10^5 g mol^{-1}, charge density: 3.5 mequiv g^{-1}] was purchased from Wako Pure Chemical Industries, Co. Ltd. Muscovite mica discs were provided by NIRACO, Co. Ltd. and HOPG by Veeco Instruments, Co. Ltd. Sodium chloride (NaCl), nickel chloride ($NiCl_2$), and calcium chloride ($CaCl_2$) were purchased from Wako. The water used in this study was purified with a Milli-Q system (Millipore, Co. Ltd.). Other chemicals were of reagent grade and used without further purification.

4.2. Sample preparation

CMC solution (1 g L^{-1}) and a series of salt solutions with designed concentrations were prepared using Milli-Q water. The working solutions were prepared by mixing these components to obtain CMC solutions (10 mg L^{-1}) containing various salts. Droplets of each solution (10 μL) were deposited onto either freshly cleaved mica or acetone-prewashed HOPG, and then left for 5 min or 3 s at room temperature, respectively, followed by rinsing with Milli-Q water and drying in a stream of dry N_2 gas.

4.3. AFM imaging

AFM topographical images were obtained under atmospheric conditions at room temperature using a NanoScope IIIa AFM apparatus (Digital Instruments, Co.

Ltd.) operated by tapping mode. Single crystal silicon cantilevers (length: 125 μm, spring constant: 40 N m^{-1}, resonance frequency: 200–400 kHz) were used. AFM measurements were carried out at five different regions (3.0×3.0 and 1.0×1.0 μm^2) per sample. The morphological features of the AFM images, that is, height and width, were analyzed using the AFM-accessory software (ver. 5.12b36). All AFM images presented here were adequately flattened using the software to correct the distortion at a micrometer scale, but no other digital operation was carried out.

Acknowledgements

This research was supported by a Grant-in-Aid for Young Scientists (No. 17688008) from the Ministry of Education, Culture, Sports, Science and Technology (MEXT), Japan.

References

1. Binning, G.; Quate, C. F.; Gerber, C. *Phys. Rev. Lett.* **1986**, *6*, 930–933.
2. Wilkinson, K. J.; Balnois, E.; Leppard, G. G.; Buffle, J. *Colloids Surf., A* **1999**, *155*, 287–310.
3. Thomson, N. H.; Kasas, S.; Smith, B.; Hansma, H. G.; Hansma, P. K. *Langmuir* **1996**, *12*, 5905–5908.
4. Kumaki, J.; Hashimoto, T. *J. Am. Chem. Soc.* **2003**, *125*, 4907–4917.
5. Capron, I.; Alexandre, S.; Muller, G. *Polymer* **1998**, *39*, 5725–5730.
6. Helen, G. H.; Daniel, E. L. *Biophys. J.* **1996**, *70*, 1933–1939.
7. Shlyakhtenko, L. S.; Gall, A. A.; Weimer, J. J.; Hawn, D. D.; Lyubchenko, Y. L. *Biophys. J.* **1999**, *77*, 568–576.
8. Podesta, A.; Imperadori, L.; Colnaghi, W.; Finzi, L.; Milani, P.; Dunlap, D. *J. Microsc.* **2004**, *215*, 236–240.
9. Adamcik, J.; Klinov, D. V.; Witz, G.; Sekatskii, S. K.; Dietler, G. *FEBS Lett.* **2006**, *580*, 5671–5675.
10. Leunissen, M. E.; Graswinckel, W. S.; van Enckevort, J. P.; Vlieg, E. *Cryst. Growth Des.* **2004**, *4*, 361–367.
11. Imase, T.; Ohira, A.; Okoshi, K.; Sano, N.; Kawauchi, S.; Watanabe, J.; Kunitake, M. *Macromolecules* **2003**, *36*, 1865–1869.
12. Percec, V.; Rudick, J. G.; Wagner, M.; Obata, M.; Mitchell, C. M.; Cho, W.; Magonov, S. N. *Macromolecules* **2006**, *39*, 7342–7351.
13. Heinze, T.; Erler, U.; Nehls, I.; Klemm, D. *Angew. Makromol. Chem.* **1994**, *215*, 93–106.
14. Khvan, A. M.; Madzhidova, V. E.; Turaev, A. S. *Chem. Nat. Compd.* **2005**, *41*, 88–90.
15. Michailova, V.; Titeva, St.; Kotsilkova, R.; Krusteva, E.; Minkov, E. *Colloids Surf., A* **1999**, *149*, 515–520.
16. Bonferoni, M. C.; Rossi, S.; Ferrari, F.; Bertoni, M.; Caramella, C. *Int. J. Pharm.* **1995**, *117*, 41–48.
17. Camesano, T. A.; Wilkinson, K. J. *Biomacromolecules* **2001**, *2*, 1184–1191.
18. Balnois, E.; Stoll, S.; Wilkinson, K. J.; Buffle, J. *Macromolecules* **2000**, *33*, 7440–7447.
19. Decho, A. W. *Carbohydr. Res.* **1999**, *315*, 330–333.
20. Liebert, T.; Hornig, S.; Hesse, S.; Heinze, T. *Macromol. Symp.* **2005**, *223*, 253–266.
21. Spagnoli, C.; Korniakov, A.; Ulman, A.; Balazs, E. A.; Lyubchenko, Y. L.; Cowman, M. K. *Carbohydr. Res.* **2005**, *340*, 929–941.
22. Kirby, A. R.; Gunning, A. P.; Morris, V. *Biopolymers* **1996**, *38*, 355–366.
23. Glennon, T. M.; Mertz, K. M. *J. Mol. Struct. (THEOCHEM)* **1997**, *395*, 157–171.
24. Palma, R.; Himmel, M. E.; Brady, J. W. *J. Phys. Chem. B* **2000**, *104*, 7228–7234.